# Supplemental Information

## Supplemental Results

### A genetic screen for TRN neurite growth defects

Previous studies had identified several components needed for proper TRN outgrowth: UNC-6/Netrin (Hedgecock *et al.*, 1990), LIN-44/Wnt proteins (Hilliard and Bargmann, 2006), and a few other signaling molecules (Du and Chalfie, 2001). To systematically search for genes involved in the regulation of neurite growth, we performed an extensive genetic screen to isolate mutants with defects in TRN neurite extension. We mutagenized a strain (TU4069) carrying the *uIs134* transgene, which allows RFP expression from the TRN-specific *mec-17* promoter, and screened the progeny of individual F1 animals representing 20,200 haploid genomes. Although we focused on isolating mutants whose TRNs had morphological defects, we also obtained mutants with abnormal numbers of fluorescently labeled cells. This screen yielded 80 mutants. We identified the phenotype-causing mutations for 62 mutants; the remaining mutants either were of low penetrance (7) or did not yield a confirmable mutation by whole genome sequencing (11). The characterized mutations represented 26 genes. Mutations in 8 genes caused the loss of TRN marker expression or its expression in extra cells, and mutations in 2 genes specifically affected the development of the postembryonic AVM and PVM neurons (Table S3); most of these mutant phenotypes were previous described and thus are not discussed here. Mutations in the remaining 16 genes resulted in various TRN neurite extension defects, which were organized into seven phenotypic categories (A-G, Table S4). This screen is likely to be near saturation because 1) the number of haploid genomes examined is 10 times the reciprocal of the average mutation rate ($5 \times 10^{-4}$) for null alleles (Brenner, 1974); and 2) nine of the ten genes represented by multiple alleles had three or more alleles.

The 16 genes whose products regulate neurite outgrowth and guidance (Table S4) encode proteins that affect either extracellular signaling to the TRNs, intracellular signaling, or effectors that are directly involved in cytoskeleton rearrangement and growth cone movement. Molecules affecting extracellular signaling include the guidance protein LIN-44/Wnt and its receptor LIN-17/Frizzled, and three proteins, UNC-23, MUA-3, and SUP-26 not acting within the TRNs. PLM neurites in *lin-44* and *lin-17* mutants failed to navigate towards the anterior (category D) because of the repellent activity of the Wnt signal (Hilliard and Bargmann, 2006; Zheng *et al.*, 2015a). *unc-23* (category G) and *mua-3* (category B) are only expressed in muscle cells (Bercher *et al.*, 2001; Papsdorf *et al.*, 2014), and their mutant phenotypes could not be rescued by TRN-specific expression of the wild-type gene. Similarly, mutations in *sup-26* (category B), which encodes a RNA-binding protein and is expressed in most somatic cells (Mapes *et al.*, 2010), could not be rescued by TRN-specific expression of the wild-type gene. We have not investigated how these molecules affect neurite outgrowth and guidance in a non-cell autonomous manner.

Genes encoding molecules that are presumably involved with intracellular signaling include *unc-51*, *mec-15*, *dsh-1*, *egl-5*, *unc-73*, and *tiam-1*. *unc-51* encodes a serine/threonine-protein kinase; mutation of *unc-51* caused general outgrowth and guidance defects (category A; Du and Chalfie, 2001). *mec-15*, which is needed for touch sensitivity (Au and Chalfie, 1989), encodes a F-box protein with WD repeats and so is likely to mediate ubiquitination and protein degradation (category E; Bounoutas *et al.*, 2009). Mutation of *mec-15* caused shortening of both PLM neurites. We previously reported that DSH-1/Dishevelled (category B) negatively modulates the activity of Wnt signaling to allow posterior outgrowth against the Wnt gradients (Zheng *et al.*, 2015a) and that *egl-5* (category B), which encodes a Abd-B-like Hox transcription factor, promotes PLM differentiation by inducing the

growth of PLM-PN and at least one downstream effector (Zheng *et al.*, 2015b). We also identified guanine nucleotide exchange factors (GEFs) [UNC-73/Trio (category E) and TIAM-1 (category B)], which controls neurite extension towards the anterior and posterior, respectively (Zheng *et al.*, 2016).

We also found several downstream effectors of directional neurite outgrowth, which are the presumed targets of extracellular and intracellular signaling. Those effectors include tubulin isotypes (MEC-7/β-tubulin, MEC-12/α-tubulin, and TBA-7/α-tubulin) and kinesin motor proteins (KLP-7 and KLP-11). Their alleles isolated in this screen are shown in Table S4.

## Supplemental Tables

Table S1. Missense mutations in human α and β tubulins that caused neurological disorders in heterozygous patients.

| Gene name | Mutation | Structural function | Corpus Callosum | Reference |
|---|---|---|---|---|
| TUBA1A | I5L | Tubulin folding | hypoplastic CC | Jansen *et al.*, 2011 |
| | E55K | Lumen-facing loop | partial ACC | Morris-Rosendahl *et al.*, 2008 |
| | T56M | Lumen-facing loop | complete ACC | Bahi-Buisson *et al.*, 2014 |
| | L70S | GTP binding | complete ACC | Cushion *et al.*, 2013 |
| | P72S | Intradimer interaction | hypoplastic CC | Bahi-Buisson *et al.*, 2014 |
| | L92V | Lumen-facing loop | complete ACC | Kumar *et al.*, 2010 |
| | N101S | GTP binding | complete ACC | Bahi-Buisson *et al.*, 2014 |
| | E113K | Lateral interaction | Normal | Bahi-Buisson *et al.*, 2014 |
| | R123C | Lateral interaction | Normal | Bahi-Buisson *et al.*, 2014 |
| | V137D | Tubulin folding | partial ACC | Kumar *et al.*, 2010 |
| | S158L | Tubulin folding | complete ACC | Bahi-Buisson *et al.*, 2014 |
| | Y161H | Lateral interaction | hypoplastic CC | Poirier *et al.*, 2013 |
| | I188L | Tubulin folding | partial ACC | Poirier *et al.*, 2007 |
| | Y210C | Intradimer interaction | hypoplastic CC | Jansen *et al.*, 2011 |
| | R214H | Intradimer interaction | complete ACC | Bahi-Buisson *et al.*, 2014 |
| | D218Y | Intradimer interaction | complete ACC | Kumar *et al.*, 2010 |
| | I219V | Intradimer interaction | partial ACC | Oegema *et al.*, 2015 |
| | V235L | Tubulin folding | hypoplastic CC | Poirier *et al.*, 2013 |
| | I238V | Tubulin folding | complete ACC | Fallet-Bianco *et al.*, 2008 |
| | D249H | Longitudinal interaction | complete ACC | Poirier *et al.*, 2007 |
| | P263T | MAP binding | complete ACC | Fallet-Bianco *et al.*, 2008 |
| | R264H | MAP binding | complete ACC | Bahi-Buisson *et al.*, 2014 |
| | R264C | MAP binding | Normal | Poirier *et al.*, 2007 |
| | A270T | Tubulin folding | complete ACC | Kumar *et al.*, 2010 |
| | L286F | Lateral interaction | complete ACC | Fallet-Bianco *et al.*, 2008 |
| | V303G | Tubulin folding | partial ACC | Lecourtois *et al.* 2010 |
| | R320H | Tubulin folding | partial ACC | Bahi-Buisson *et al.*, 2014 |
| | K326N | Longitudinal interaction | complete ACC | Bahi-Buisson *et al.*, 2014 |
| | N329S | Longitudinal interaction | complete ACC | Kumar *et al.*, 2010 |
| | A333V | Longitudinal interaction | hypoplastic CC | Cushion *et al.*, 2013 |
| | V353I | Longitudinal interaction | partial ACC | Bahi-Buisson *et al.*, 2014 |
| | G366R | Lumen-facing loop | partial ACC | Okumura *et al.* 2013 |
| | A369T | Lumen-facing loop | hypoplastic CC | Bahi-Buisson *et al.*, 2014 |

| | | | | |
|---|---|---|---|---|
| | V371E | Lumen-facing loop | complete ACC | Bahi-Buisson *et al.*, 2014 |
| | M377V | Tubulin folding | partial ACC | Kumar *et al.*, 2010 |
| | A387V | MAP binding | hypoplastic CC | Romaniello *et al.*, 2012 |
| | R390C | MAP binding | complete ACC | Kumar *et al.*, 2010 |
| | R390H | MAP binding | partial ACC | Zanni *et al.* 2013 |
| | D396Y | MAP binding | partial ACC | Bahi-Buisson *et al.*, 2014 |
| | L397P | MAP binding | partial ACC | Bahi-Buisson *et al.*, 2008 |
| | R402L | MAP binding | mild hypoplastic CC | Sohal *et al.*, 2012 |
| | R402C | MAP binding | normal | Kumar *et al.*, 2010 |
| | R402H | MAP binding | normal | Kumar *et al.*, 2010 |
| | V409A | MAP binding | complete ACC | Bahi-Buisson *et al.*, 2014 |
| | V409I | MAP binding | hypoplastic CC | Bahi-Buisson *et al.*, 2014 |
| | S419L | MAP binding | partial ACC | Poirier *et al.*, 2007 |
| | R422H | MAP binding | partial ACC | Kumar *et al.*, 2010 |
| | R422C | MAP binding | hypoplastic CC | Bahi-Buisson *et al.*, 2008 |
| | M425K | MAP binding | complete ACC | Kumar *et al.*, 2010 |
| | E429Q | MAP binding | complete ACC | Bahi-Buisson *et al.*, 2014 |
| | G436R | MAP binding | hypoplastic CC | Bahi-Buisson *et al.*, 2008 |
| TUBB2B | G13A | Tubulin folding | normal | Oegema *et al.*, 2015 |
| | G98R | GTP binding | complete ACC | Cushion *et al.*, 2013 |
| | L117P | Tubulin folding | normal | Guerrini *et al.*, 2012 |
| | G140A | GTP binding | complete ACC | Romaniello *et al.*, 2012 |
| | P171T | GTP binding | partial ACC | Bahi-Buisson *et al.*, 2014 |
| | S172P | GTP binding | complete ACC | Jaglin *et al.*, 2009 |
| | P173L | GTP binding | complete ACC | Bahi-Buisson *et al.*, 2014 |
| | I202T | Tubulin folding | partial ACC | Bahi-Buisson *et al.*, 2014 |
| | L207P | Tubulin folding | complete ACC | Cushion *et al.*, 2013 |
| | I210T | Tubulin folding | partial ACC | Jaglin *et al.*, 2009 |
| | L228P | Tubulin folding | complete ACC | Jaglin *et al.*, 2009 |
| | C239F | Intradimer interaction | complete ACC | Bahi-Buisson *et al.*, 2014 |
| | R241H | Intradimer interaction | normal | Bahi-Buisson *et al.*, 2014 |
| | A248T | Intradimer interaction | normal | Bahi-Buisson *et al.*, 2014 |
| | D249H | Intradimer interaction | complete ACC | Bahi-Buisson *et al.*, 2014 |
| | N256S | Intradimer interaction | hypoplastic CC | Guerrini *et al.*, 2012 |
| | F265L | Tubulin folding | partial ACC | Jaglin *et al.*, 2009 |
| | S278G | Lateral interaction | partial ACC | Bahi-Buisson *et al.*, 2014 |
| | T312M | Tubulin folding | hypoplastic CC | Jaglin *et al.*, 2009 |
| | G369V | Lumen-facing loop | partial ACC | Bahi-Buisson *et al.*, 2014 |

| | | | | |
|---|---|---|---|---|
| | R380S | MAP binding | complete ACC | Cushion *et al.*, 2013 |
| | R380C | MAP binding | complete ACC | Cushion *et al.*, 2013 |
| | R380L | MAP binding | complete ACC | Amrom *et al.*, 2014 |
| | D417N | MAP binding | normal | Guerrini *et al.*, 2012 |
| TUBB3 | R46G | Intradimer interaction | hypoplastic CC | Bahi-Buisson *et al.*, 2014 |
| | R62Q | Tubulin folding | normal | Tischfield *et al.*, 2010 |
| | G71R | Tubulin folding | partial ACC | Whitman *et al.*, 2016 |
| | G82R | Tubulin folding | partial ACC | Poirier *et al.*, 2010 |
| | G98S | Longitudinal interaction | hypoplastic CC | Whitman *et al.*, 2016 |
| | T178M | GTP binding | complete ACC | Poirier *et al.*, 2010 |
| | E205K | Tubulin folding | hypoplastic CC | Poirier *et al.*, 2010 |
| | R262C | MAP binding | partial ACC | Tischfield *et al.*, 2010 |
| | R262H | MAP binding | partial ACC | Tischfield *et al.*, 2010 |
| | E288K | Lateral interaction | hypoplastic CC | Oegema *et al.*, 2015 |
| | A302T | MAP binding | partial ACC | Tischfield *et al.*, 2010 |
| | A302V | MAP binding | hypoplastic CC | Poirier *et al.*, 2010 |
| | M323V | Intradimer interaction | partial ACC | Poirier *et al.*, 2010 |
| | P357L | Tubulin folding | normal | Oegema *et al.*, 2015 |
| | R380C | MAP binding | partial ACC | Tischfield *et al.*, 2010 |
| | M388V | MAP binding | complete ACC | Poirier *et al.*, 2010 |
| | E410K | MAP binding | partial ACC | Tischfield *et al.*, 2010 |
| | D417N | MAP binding | partial ACC | Tischfield *et al.*, 2010 |
| | D417H | MAP binding | N/A | Tischfield *et al.*, 2010 |

51 TUBA1A, 24 TUBB2B, and 19 TUBB3B mutations are listed. The mutated amino acids were mapped to the structural domains of α/β heterodimer and their potential structural functions were assigned according to Tischfield *et al.* (2011). Residues located in the interior of the structure were generally assigned to the category of "tubulin folding." Effects on the corpus callosum (CC) were used as an indicator of defects in axon growth and guidance. These phenotypes were extracted from the cited literature. ACC stands for agenesis of the corpus callosum.

Table S2. Loss-of-function alleles of α and β tubulin genes (other than *mec-12* and *mec-7*) and their effects on TRN morphology.

| **Gene** | **Allele** | **TRN morphology** |
|---|---|---|
| *tba-1* | *ok1123* | Normal |
| *tba-1* | *ok1135* | Normal |
| *tba-1* | *or346* | Normal |
| *tba-1* | *or594* | Normal |
| *tba-2* | *sb51* | Normal |
| *tba-2* | *sb25* | Normal |
| *tba-5* | *tm4200* | Normal |
| *tba-7* | *gk787939* | Ectopic ALM-PN |
| *tba-7* | *u1015* | Ectopic ALM-PN |
| *tba-8* | *tm4359* | Normal |
| *tba-9* | *ok1858* | Normal |
| *ben-1* | *e1880* | Normal |
| *tbb-1* | *gk207* | Normal |
| *tbb-2* | *t1623* | Normal |
| *tbb-2* | *gk130* | Normal |
| *tbb-4* | *sa127* | Normal |
| *tbb-4* | *ok1461* | Normal |
| *tbb-6* | *tm2004* | Normal |

Table S3. Mutations that affect the expression pattern of TRN marker or the development of the postembryonic AVM and PVM cells.

| | **Gene name** | **Allele name** | **Phenotype** | **Recessivity** | **Penetr-ance** | **Molecular Lesion** | **Reference** |
|---|---|---|---|---|---|---|---|
| i | Mutations resulting in the absence of TRN maker | | | | | | |
| | *lin-32* | *u909* | Lack of PLM, AVM, and PVM labeling | recessive | 58% | | Mitani *et al.*, 1993 |
| | *cdk-4* | *u948* | Lack of PLM, AVM, and PVM labeling | recessive | 88% | Q18* | |
| | *mec-4* | *u947; u972* | Degeneration of TRNs | recessive | 35% *(u947)* | A513T | |
| | | *u951* | Degeneration of TRNs | dominant | 65% | A713T | Driscoll and Chalfie, 1991 |
| | *mec-10* | *u1025* | Degeneration of TRNs | recessive | 10% | G312R | |
| ii | Mutations resulting in the expression of TRN markers in extra cells | | | | | | |
| | *egl-46* | *u945* | Expression of TRN marker in FLPs | recessive | 65% | | Wu *et al.*, 2001 |
| | *egl-44* | *u965* | Expression of TRN marker in FLPs | recessive | 79% | | Wu *et al.*, 2001 |
| | *pag-3* | *u920; u949; u961* | Expression of TRN marker in BDUs | recessive | 90% (*u920*) | | Jia *et al.*, 1996 |
| | *egl-13* | *u964* | Expression of TRN marker in A/PQRs | recessive | 68% | H389Y | Feng *et al.*, 2013 |
| iii | Mutations resulting in developmental defects in AVM/PVM | | | | | | |
| | *egl-20* | *u999* | PVM is mispositioned anteriorly | recessive | 82% | V92D | Harris *et al.*, 1996 |
| | *unc-6* | *u1018* | Ventral guidance defects for AVM neurites | recessive | 61% | C346Y | Hedgecock *et al.*, 1990 |

References indicate that similar mutant phenotypes for the gene were previously reported. *cdk-4* was not previously known to affect TRN development. Although they each have the same underlying defect, *u947* and *u972* were independently isolated. These two alleles and *mec-10(u1025)* identify novel changes that cause TRN degeneration.

Table S4. Mutations that cause neurite outgrowth or guidance defects in TRNs.

| | **Gene name** | **Allele name** | **Recessivity** | **Penet-rance** | **Molecular Lesion** | **Reference** |
|---|---|---|---|---|---|---|
| A | Mutations that shorten all TRN neurites | | | | | |
| | *mec-7* | *u910* | dominant | 100% | P356L | |
| | | *u911* | dominant | | P171S | |
| | | *u955* | dominant | | A352T | |
| | | *u956* | dominant | | P358L | |
| | | *u957* | dominant | | P171L | |
| | | *u958* | dominant | | G244S | |
| | *unc-51* | *u1000* | recessive | 80% | E188K | Du and Chalfie, 2001 |
| B | Mutations that shorten the PLM-PN | | | | | |
| | *mec-7* | *u1020* | recessive | | G34S | |
| | *mec-12* | *u1019* | dominant | | G354E | |
| | | *u950* | recessive | | S140F | |
| | | *u1016* | recessive | | E97K | |
| | | *u1021* | recessive | | G144S | |
| | *dsh-1* | *u915* | recessive | 95% | R165Stop | Zheng *et al.*, 2015a |
| | | *u952* | recessive | | G512R | |
| | | *u953* | recessive | | R103Stop | |
| | *tiam-1* | *u914* | recessive | 98% | R570Stop | Zheng *et al.*, 2016 |
| | | *u1003* | recessive | | | |
| | | *u1004* | recessive | | R420Stop | |
| | | *u1005* | recessive | | Q846Stop | |
| | | *u1012* | recessive | | Q266Stop | |
| | *egl-5* | *u918; u966* | recessive | 100% | | Zheng *et al.*, 2015b |
| | *mua-3* | *u973* | recessive | 45% | C2191Y | |
| | *sup-26* | *u916* | recessive | 81% | G95Stop | |
| C | Mutations that result in an ectopic ALM-PN | | | | | |
| | *mec-12* | *u917* | recessive | 38% | V260I | |
| | *mec-7* | *u1017* | recessive | 83% | L377F | |
| | *tba-7* | *u1015* | recessive | 79% | G92D | |
| D | Mutations that shorten PLM-AN and elongate PLM-PN | | | | | |
| | *lin-44* | *u905; u906; u907; u959* | recessive | 90% *(u905)* | | Hilliard and Bargmann, 2006; Zheng *et al.*, 2015a |
| | *lin-17* | *u919; u960; u962; u963* | recessive | 75% *(u919)* | | Hilliard and Bargmann, 2006; Zheng *et al.*, 2015a |
| E | Mutations that shorten both PLM-AN and PLM-PN | | | | | |
| | *mec-15* | *u1008* | recessive | 83% | Q194Stop | |
| F | Mutations that shorten ALM-AN and PLM-AN | | | | | |
| | *unc-73* | *u908* | recessive | 85% | E1212K | Du and Chalfie, 2001; Zheng *et al.*, 2016 |

| | | | | | | |
|---|---|---|---|---|---|---|
| | *unc-53* | *u913* | recessive | 90% | Q261Stop | Hekimi and Kershaw, 1993 |
| | | *u912; u946; u967; u968; u969; u970; u971; u974* | recessive | | | |
| | *klp-11* | *u1024* | recessive | 79% | Q53Stop | |
| G | Mutations that shorten ALM-AN but not PLM-AN | | | | | |
| | *unc-23* | *u1022* | recessive | 82% | Q132Stop | |

References indicate that the similar mutant phenotypes for the gene were either previously reported or we extensively characterized the mutants elsewhere.

**Supplemental Figures**

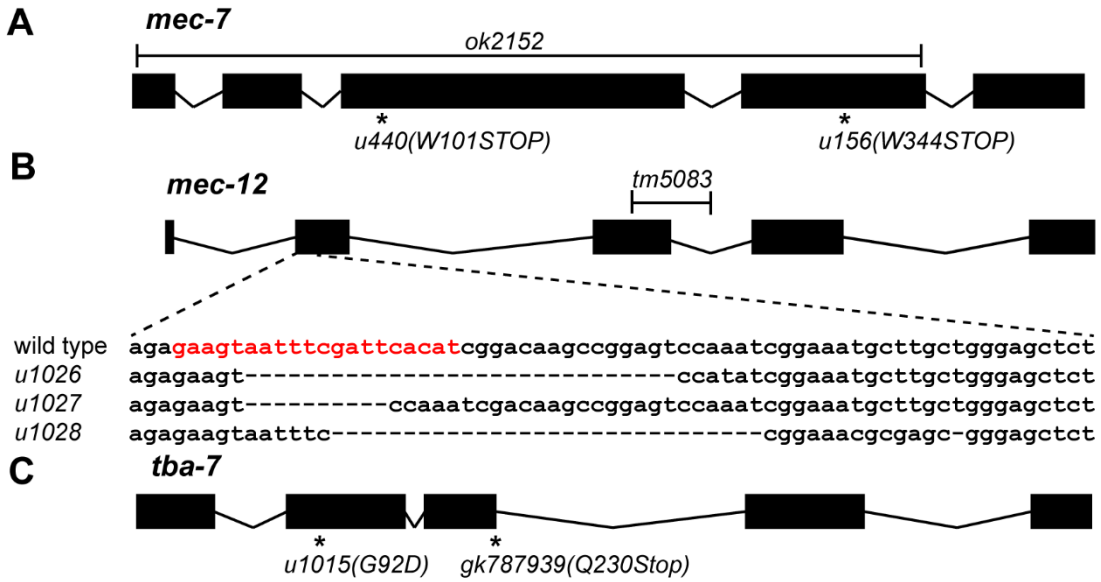


Figure S1. Gene structures for *mec-7*, *mec-12*, and *tba-7* and the molecular lesions in various putative null alleles. *u1026*, *u1027*, and *u1028* were created using CRISPR/Cas9-mediated genome editing and guide RNAs designed to target exon 2 of *mec-12*. Frameshift-causing deletions were identified by genotyping. The *tm5083* mutation deletes part of exon 3 and intron 3 of *mec-12* and also causes a frameshift.

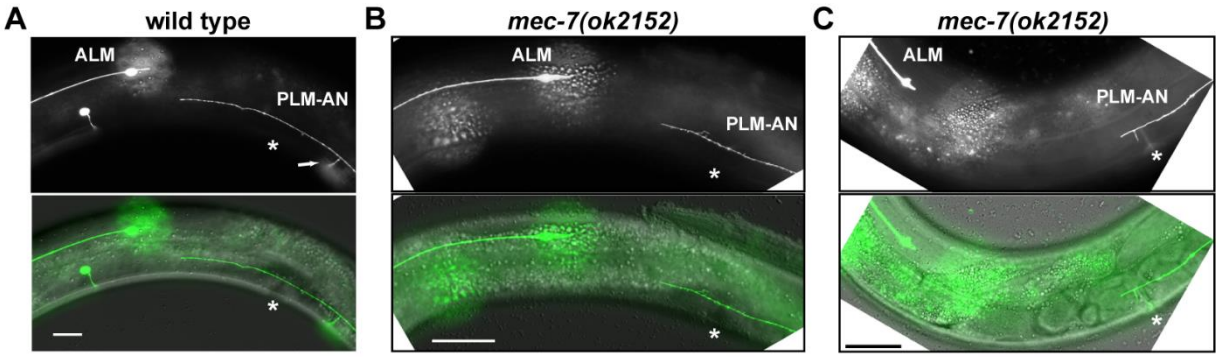


Figure S2. The loss of MEC-7 causes PLM-AN branching defects. *uIs31[mec-17p::GFP]* was used to examine the TRN morphology. (A) In the wild-type animals, PLM-AN extends beyond the vulva (asterisk) and sends out a synaptic branch at a position posterior to the vulva; the branch extends to reach the ventral nerve cord. (B-C) PLM-AN is slightly shorter in *mec-7 (ok2152lf)* animals, although it still extends beyond the vulva (asterisk). However, PLM-AN fails to form a synaptic branch (B) or could not fully extend the branch at the correct position (C). Scale bar = 20 μm.

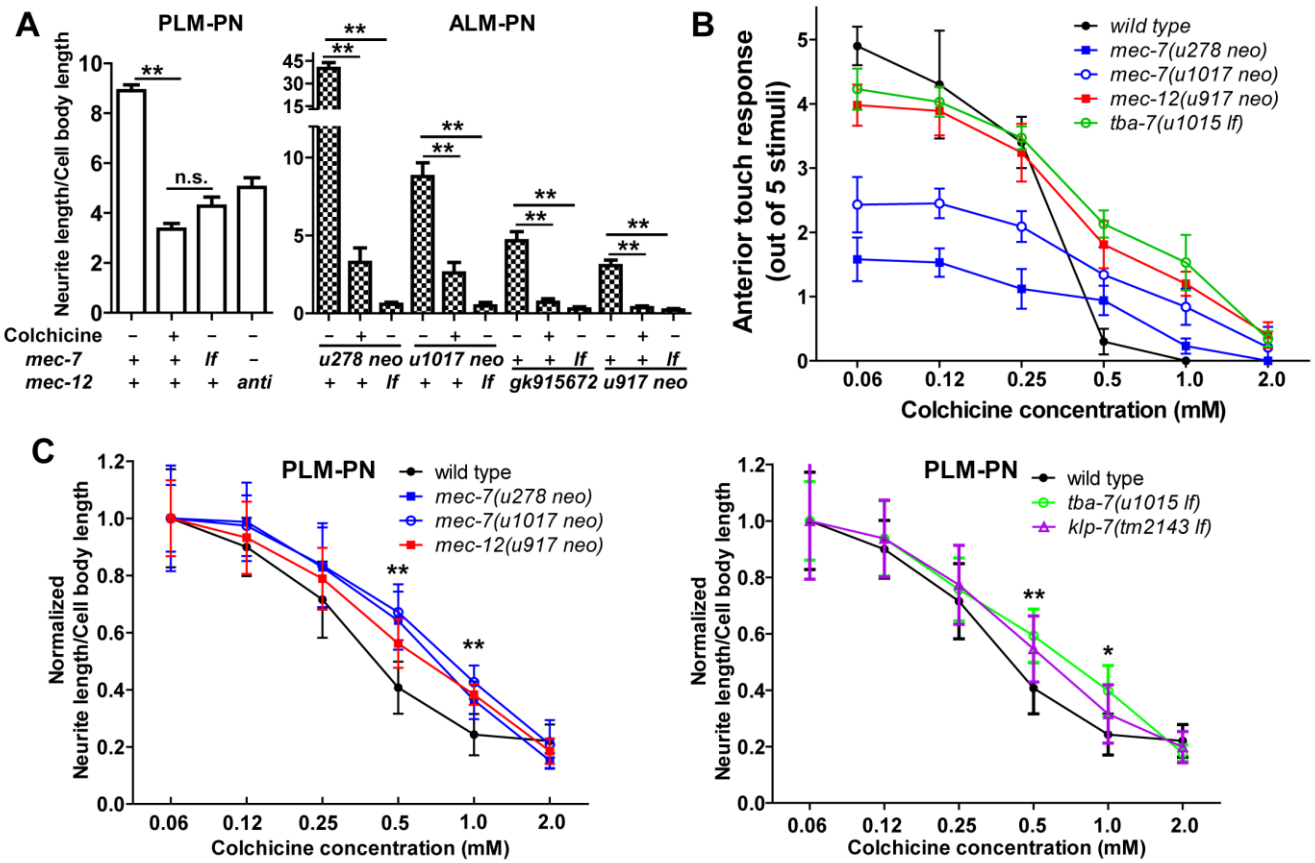


Figure S3. *mec-7(neo)* and *mec-12(neo)*, *tba-7(lf)*, and *klp-7(lf)* mutants have increased resistance to colchicine. (A) The comparison of PLM-PN length in wild type animals treated with 1 mM colchicine with *mec-7(ok2152 lf)* and *mec-12(u1021 anti)* mutants. (B) Anterior touch response of adult animals grown on plate containing different concentrations of colchicine from the first larval (L1) stage. (C) The normalized length of PLM-PN of adults grown on plates with colchicine from the L1 stage. PLM-PN lengths of animals treated with 0.06 mM colchicine (9.0 for wild type, 13.3 for *u278*, 10.0 for *u1017*, 10.1 for *u917*, 11.0 for *u1015*, and 10.5 for *tm2143*) were used to set as the reference for the normalization. Asterisks indicate the differences among the means were statistically significant in ANOVA tests (one asterisk indicates $p < 0.05$ and two for $p < 0.01$).

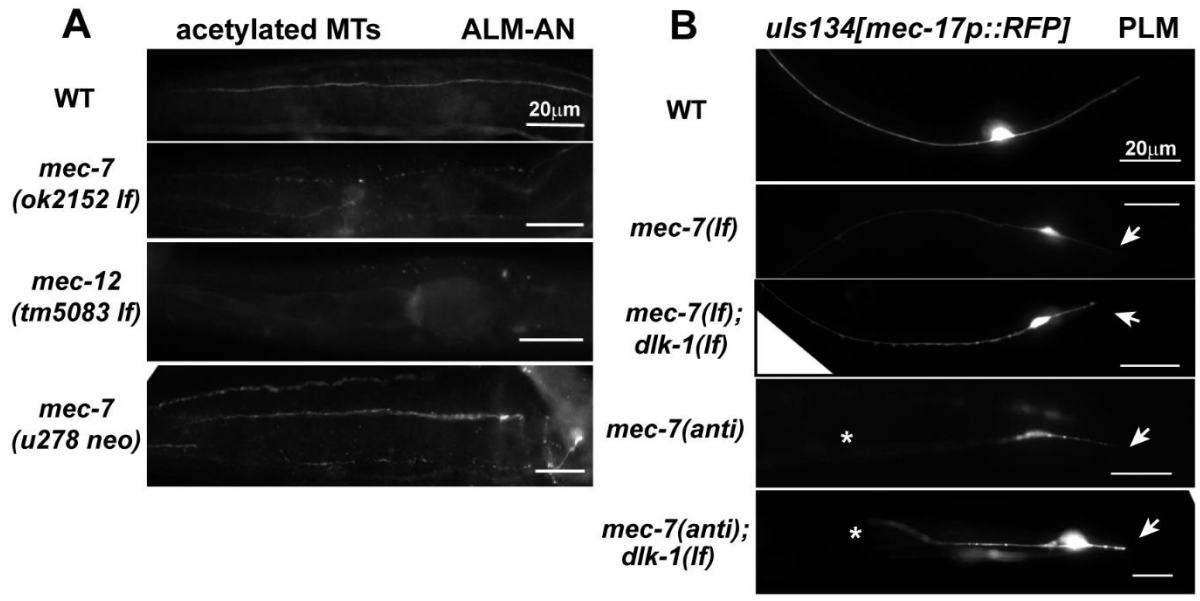


Figure S4. MT acetylation and RFP fluorescence in *mec-7* and *mec-12* mutants. (A) Representative images of ALM-AN stained by anti-acetylated α-tubulin antibodies [6-11B-1] in the wild type animals and the indicated mutants. (B) The fluorescent intensity of RFP expressed from the transgene *uIs134[mec-17p::GFP]* in the wild type animal, *mec-7(ok2152 lf)* mutants, and *mec-7(ok2152 lf); dlk-1(ju476)* double mutants, as well as *mec-7(u957 anti)* mutants and *mec-7(u957 anti); dlk-1(ju476)* double mutants. Images were collected using the same exposure time and laser intensity to allow the comparison of fluorescent intensity. *dlk-1* mutation enhanced RFP level in the *mec-7* mutants but did not rescue the neurite growth defects. Arrows point to the shortened PLM-PN and asterisks indicate the terminating position of the shortened PLM-AN. Scale bar = 20 μm.

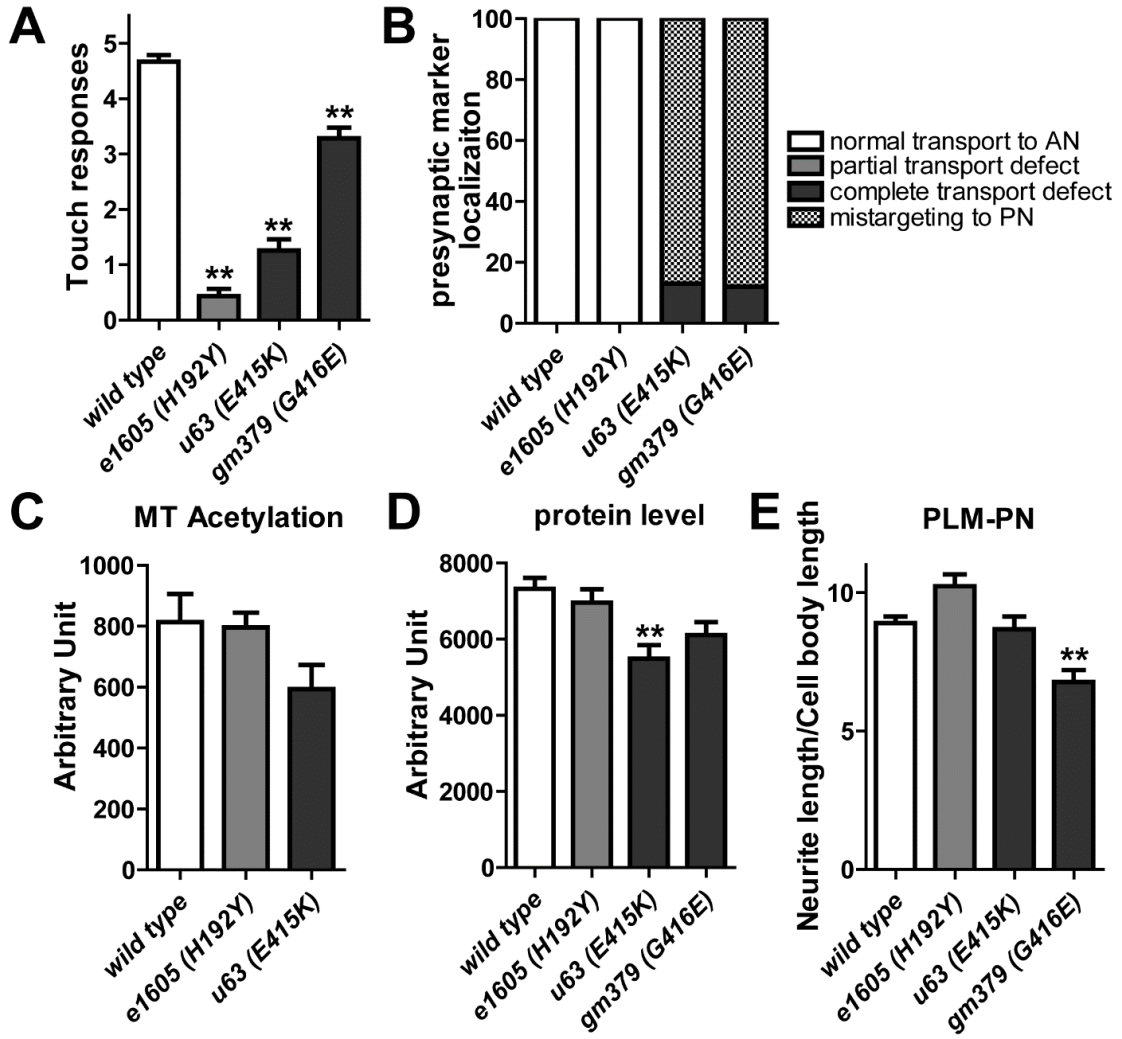


Figure S5. *mec-12* alleles that specifically affect touch sensitivity or synaptic vesicle transport. (A) Anterior touch response (out of five stimuli) of the *mec-12* alleles. (B) Percentage of PLM cells showing transport defects or mistargeting of the presynaptic marker RAB-3::GFP. (C) Immunofluorescent intensity of staining using anti-acetylated α-tubulin antibodies. (D) Fluorescent intensity of RFP expressed from the transgene *uIs134[mec-17p::RFP]* crossed into the *mec-12* mutants. Arbitrary units were used in C and D. (E) The length of the PLM-PN in some *mec-12* mutants. Asterisks indicate significant differences ($p < 0.01$) from the wild type animals.

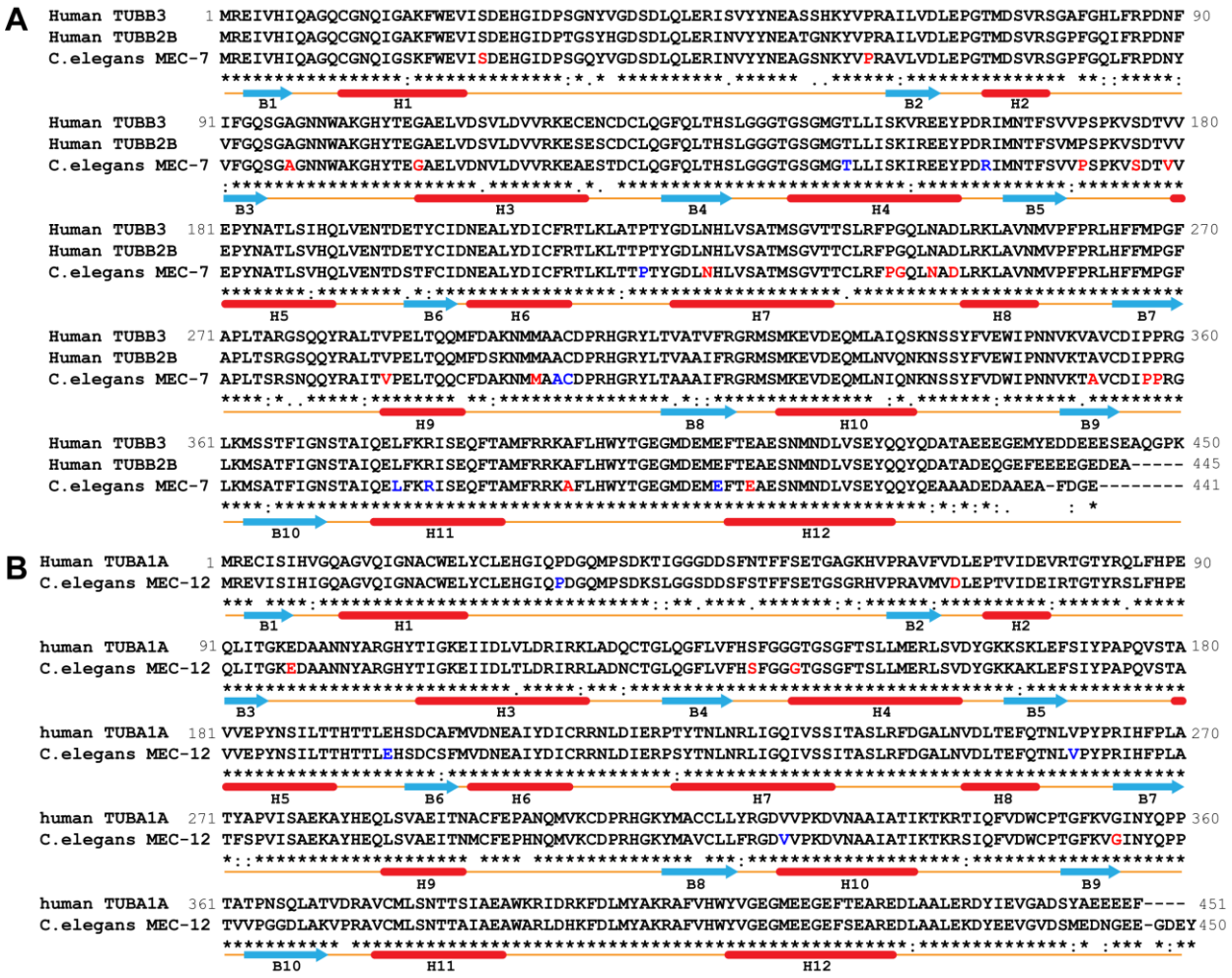


Figure S6. Sequence alignment of MEC-7 with human TUBB3 and TUBB2B (A) and alignment between MEC-12 and TUBA1A (B). Regions predicted to be α-helices (H1 to H12) or β-strands (B1 to B10) by the α/β tubulin dimer structure (1jff.pdb; Nogales *et al.*, 1998) were labeled. Amino acids that were changed in *mec-7* or *mec-12 anti* and *neo* mutants were labeled in red and blue, respectively.

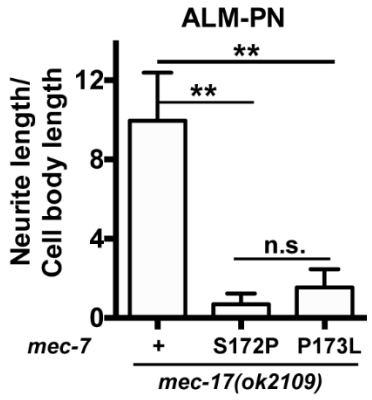


Figure S7. Both *mec-7[u1056* (S172P)*]* and *mec-7[u1057* (P173L)*]* mutation suppressed the growth of ALM-PN in *mec-17(ok2109 lf)* mutants.

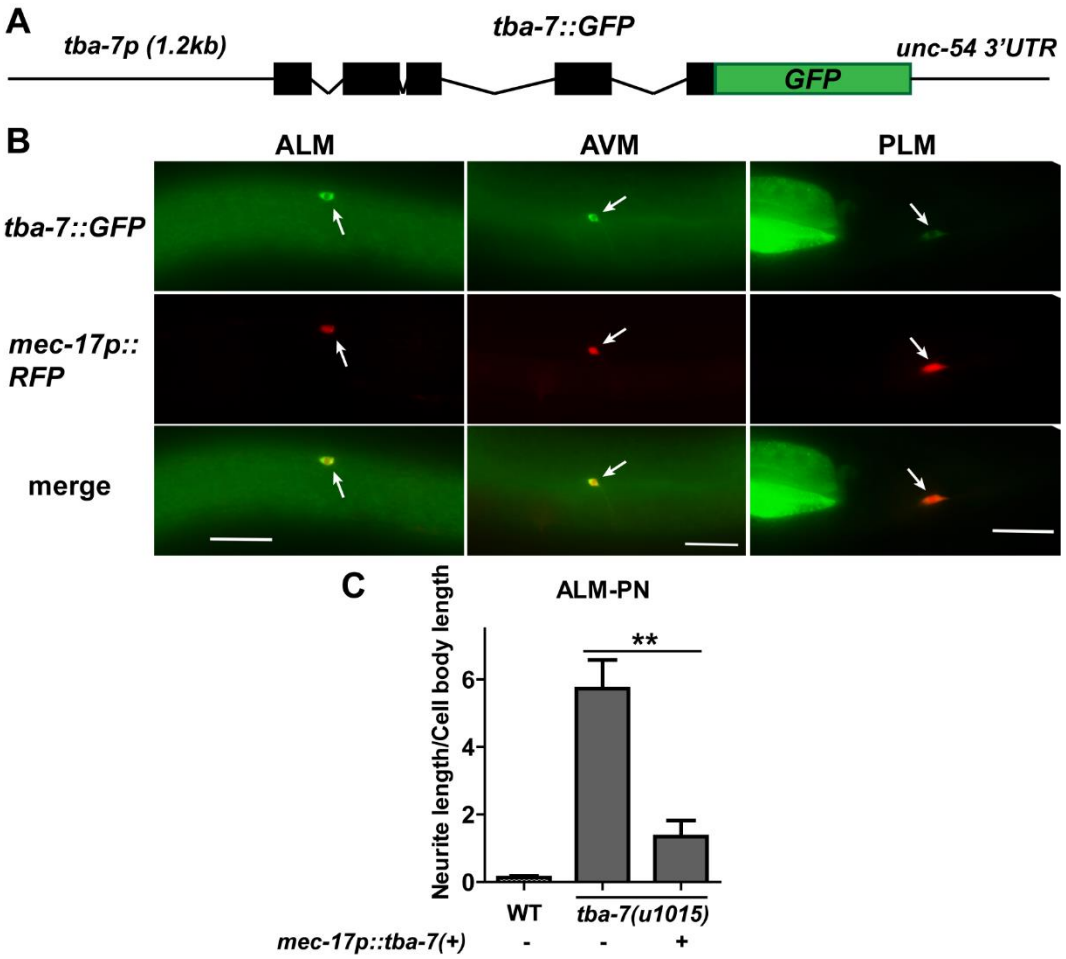


Figure S8. TBA-7 is expressed and acts cell-autonomously in the TRNs. (A) A schematic representation of the *tba-7::GFP* reporter, containing a 1.2 kb promoter and the entire coding region. (B) The expression of *tba-7::GFP* in the TRNs, which are also labeled by *mec-17p::RFP*. Arrows point to the cell bodies of TRNs. The posterior intestine also showed strong GFP signal (the rightmost panel). (C) The length of ALM-PN in *tba-7(u1015 lf)* mutants that carried a rescuing array that expressed wild-type *tba-7* in the TRNs specifically.

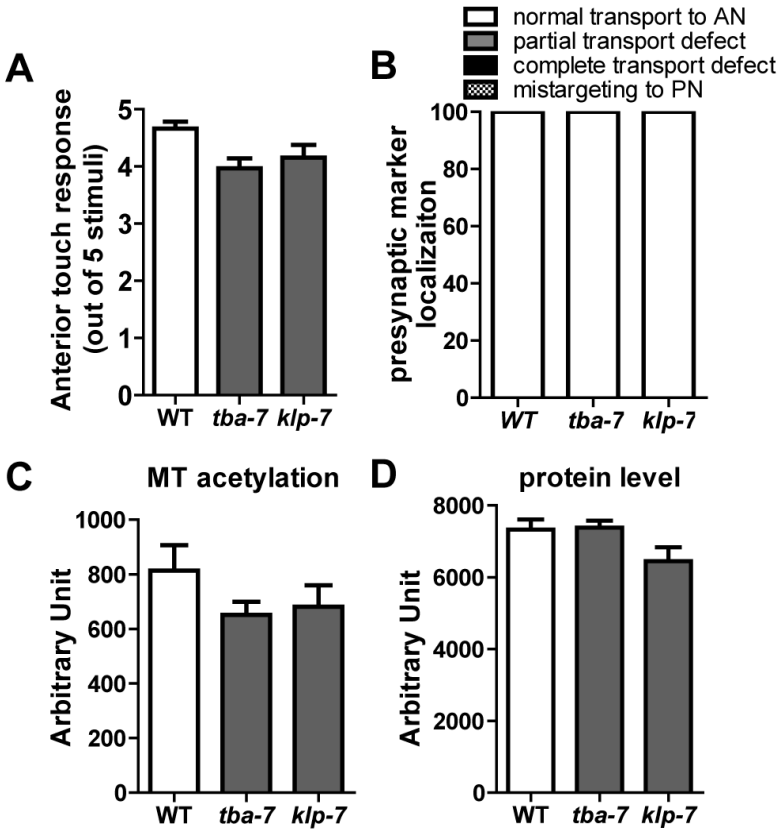


Figure S9. Touch sensitivity, presynaptic vesicle localization, tubulin acetylation level, and protein expression level of *tba-7(u1015 lf)* and *klp-7(tm2143 lf)* mutants. No significant differences between these mutants and wild type were found.

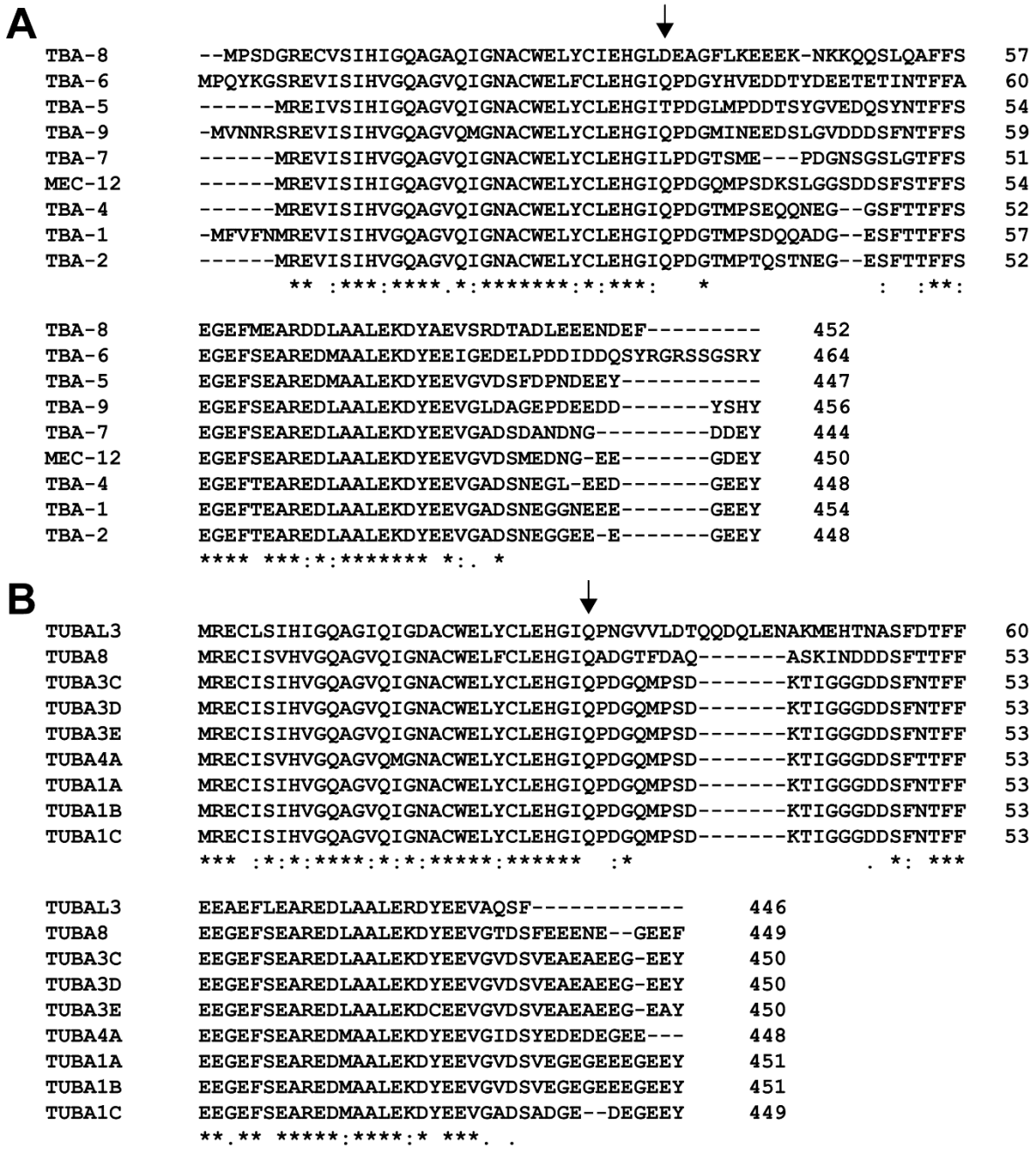


Figure S10. Sequence alignment of all *C. elegans* α-tubulin proteins (A) and all human α-tubulin proteins (B). Only the N-terminal and C-terminal sequences were shown. The arrow points to Q31 residue.

## References


Amrom, D., Tanyalcin, I., Verhelst, H., Deconinck, N., Brouhard, G.J., Decarie, J.C., Vanderhasselt, T., Das, S., Hamdan, F.F., Lissens, W., Michaud, J.L., and Jansen, A.C. (2014). Polymicrogyria with dysmorphic basal ganglia? Think tubulin! Clin Genet *85*, 178-183.

Bahi-Buisson, N., Poirier, K., Boddaert, N., Saillour, Y., Castelnau, L., Philip, N., Buyse, G., Villard, L., Joriot, S., Marret, S., Bourgeois, M., Van Esch, H., Lagae, L., Amiel, J., Hertz-Pannier, L., Roubertie, A., Rivier, F., Pinard, J.M., Beldjord, C., and Chelly, J. (2008). Refinement of cortical dysgeneses spectrum associated with TUBA1A mutations. J Med Genet *45*, 647-653.

Bahi-Buisson, N., Poirier, K., Fourniol, F., Saillour, Y., Valence, S., Lebrun, N., Hully, M., Bianco, C.F., Boddaert, N., Elie, C., Lascelles, K., Souville, I., Consortium, L.I.-T., Beldjord, C., and Chelly, J. (2014). The wide spectrum of tubulinopathies: what are the key features for the diagnosis? Brain *137*, 1676-1700.

Bercher, M., Wahl, J., Vogel, B.E., Lu, C., Hedgecock, E.M., Hall, D.H., and Plenefisch, J.D. (2001). mua-3, a gene required for mechanical tissue integrity in Caenorhabditis elegans, encodes a novel transmembrane protein of epithelial attachment complexes. J Cell Biol *154*, 415-426.

Bounoutas, A., Zheng, Q., Nonet, M.L., and Chalfie, M. (2009). mec-15 encodes an F-box protein required for touch receptor neuron mechanosensation, synapse formation and development. Genetics *183*, 607-617, 601SI-604SI.

Brenner, S. (1974). The genetics of Caenorhabditis elegans. Genetics *77*, 71-94.

Cushion, T.D., Dobyns, W.B., Mullins, J.G., Stoodley, N., Chung, S.K., Fry, A.E., Hehr, U., Gunny, R., Aylsworth, A.S., Prabhakar, P., Uyanik, G., Rankin, J., Rees, M.I., and Pilz, D.T. (2013). Overlapping cortical malformations and mutations in TUBB2B and TUBA1A. Brain *136*, 536-548.

Driscoll, M., and Chalfie, M. (1991). The mec-4 gene is a member of a family of Caenorhabditis elegans genes that can mutate to induce neuronal degeneration. Nature *349*, 588-593.

Du, H., and Chalfie, M. (2001). Genes regulating touch cell development in Caenorhabditis elegans. Genetics *158*, 197-207.

Fallet-Bianco, C., Loeuillet, L., Poirier, K., Loget, P., Chapon, F., Pasquier, L., Saillour, Y., Beldjord, C., Chelly, J., and Francis, F. (2008). Neuropathological phenotype of a distinct form of lissencephaly associated with mutations in TUBA1A. Brain *131*, 2304-2320.

Feng, G., Yi, P., Yang, Y., Chai, Y., Tian, D., Zhu, Z., Liu, J., Zhou, F., Cheng, Z., Wang, X., Li, W., and Ou, G. (2013). Developmental stage-dependent transcriptional regulatory pathways control neuroblast lineage progression. Development *140*, 3838-3847.

Guerrini, R., Mei, D., Cordelli, D.M., Pucatti, D., Franzoni, E., and Parrini, E. (2012). Symmetric polymicrogyria and pachygyria associated with TUBB2B gene mutations. Eur J Hum Genet *20*, 995-998.

Harris, J., Honigberg, L., Robinson, N., and Kenyon, C. (1996). Neuronal cell migration in C. elegans: regulation of Hox gene expression and cell position. Development *122*, 3117-3131.

Hedgecock, E.M., Culotti, J.G., and Hall, D.H. (1990). The unc-5, unc-6, and unc-40 genes guide circumferential migrations of pioneer axons and mesodermal cells on the epidermis in C. elegans. Neuron *4*, 61-85.

Hekimi, S., and Kershaw, D. (1993). Axonal guidance defects in a Caenorhabditis elegans mutant reveal cell-extrinsic determinants of neuronal morphology. The Journal of neuroscience : the official journal of the Society for Neuroscience *13*, 4254-4271.

Hilliard, M.A., and Bargmann, C.I. (2006). Wnt signals and frizzled activity orient anterior-posterior axon outgrowth in C. elegans. Developmental cell *10*, 379-390.
Jaglin, X.H., Poirier, K., Saillour, Y., Buhler, E., Tian, G., Bahi-Buisson, N., Fallet-Bianco, C., Phan-Dinh-Tuy, F., Kong, X.P., Bomont, P., Castelnau-Ptakhine, L., Odent, S., Loget, P., Kossorotoff, M., Snoeck, I., Plessis, G., Parent, P., Beldjord, C., Cardoso, C., Represa, A., Flint, J., Keays, D.A., Cowan, N.J., and Chelly, J. (2009). Mutations in the beta-tubulin gene TUBB2B result in asymmetrical polymicrogyria. Nat Genet *41*, 746-752.
Jansen, A.C., Oostra, A., Desprechins, B., De Vlaeminck, Y., Verhelst, H., Regal, L., Verloo, P., Bockaert, N., Keymolen, K., Seneca, S., De Meirleir, L., and Lissens, W. (2011). TUBA1A mutations: from isolated lissencephaly to familial polymicrogyria. Neurology *76*, 988-992.
Jia, Y., Xie, G., and Aamodt, E. (1996). pag-3, a Caenorhabditis elegans gene involved in touch neuron gene expression and coordinated movement. Genetics *142*, 141-147.
Kumar, R.A., Pilz, D.T., Babatz, T.D., Cushion, T.D., Harvey, K., Topf, M., Yates, L., Robb, S., Uyanik, G., Mancini, G.M., Rees, M.I., Harvey, R.J., and Dobyns, W.B. (2010). TUBA1A mutations cause wide spectrum lissencephaly (smooth brain) and suggest that multiple neuronal migration pathways converge on alpha tubulins. Hum Mol Genet *19*, 2817-2827.
Lecourtois, M., Poirier, K., Friocourt, G., Jaglin, X., Goldenberg, A., Saugier-Veber, P., Chelly, J., and Laquerriere, A. (2010). Human lissencephaly with cerebellar hypoplasia due to mutations in TUBA1A: expansion of the foetal neuropathological phenotype. Acta Neuropathol *119*, 779-789.
Mapes, J., Chen, J.T., Yu, J.S., and Xue, D. (2010). Somatic sex determination in Caenorhabditis elegans is modulated by SUP-26 repression of tra-2 translation. Proceedings of the National Academy of Sciences of the United States of America *107*, 18022-18027.
Mitani, S., Du, H., Hall, D.H., Driscoll, M., and Chalfie, M. (1993). Combinatorial control of touch receptor neuron expression in Caenorhabditis elegans. Development *119*, 773-783.
Morris-Rosendahl, D.J., Najm, J., Lachmeijer, A.M., Sztriha, L., Martins, M., Kuechler, A., Haug, V., Zeschnigk, C., Martin, P., Santos, M., Vasconcelos, C., Omran, H., Kraus, U., Van der Knaap, M.S., Schuierer, G., Kutsche, K., and Uyanik, G. (2008). Refining the phenotype of alpha-1a Tubulin (TUBA1A) mutation in patients with classical lissencephaly. Clin Genet *74*, 425-433.
Nogales, E., Wolf, S.G., and Downing, K.H. (1998). Structure of the alpha beta tubulin dimer by electron crystallography. Nature *391*, 199-203.
Oegema, R., Cushion, T.D., Phelps, I.G., Chung, S.K., Dempsey, J.C., Collins, S., Mullins, J.G., Dudding, T., Gill, H., Green, A.J., Dobyns, W.B., Ishak, G.E., Rees, M.I., and Doherty, D. (2015). Recognizable cerebellar dysplasia associated with mutations in multiple tubulin genes. Hum Mol Genet *24*, 5313-5325.
Okumura, A., Hayashi, M., Tsurui, H., Yamakawa, Y., Abe, S., Kudo, T., Suzuki, R., Shimizu, T., Shimojima, K., and Yamamoto, T. (2013). Lissencephaly with marked ventricular dilation, agenesis of corpus callosum, and cerebellar hypoplasia caused by TUBA1A mutation. Brain Dev *35*, 274-279.
Papsdorf, K., Sacherl, J., and Richter, K. (2014). The balanced regulation of Hsc70 by DNJ-13 and UNC-23 is required for muscle functionality. The Journal of biological chemistry *289*, 25250-25261.
Poirier, K., Keays, D.A., Francis, F., Saillour, Y., Bahi, N., Manouvrier, S., Fallet-Bianco, C., Pasquier, L., Toutain, A., Tuy, F.P., Bienvenu, T., Joriot, S., Odent, S., Ville, D., Desguerre, I., Goldenberg, A., Moutard, M.L., Fryns, J.P., van Esch, H., Harvey, R.J., Siebold, C., Flint, J., Beldjord, C., and Chelly, J. (2007). Large spectrum of lissencephaly and pachygyria phenotypes resulting from de novo missense mutations in tubulin alpha 1A (TUBA1A). Hum Mutat *28*, 1055-1064.

Poirier, K., Saillour, Y., Bahi-Buisson, N., Jaglin, X.H., Fallet-Bianco, C., Nabbout, R., Castelnau-Ptakhine, L., Roubertie, A., Attie-Bitach, T., Desguerre, I., Genevieve, D., Barnerias, C., Keren, B., Lebrun, N., Boddaert, N., Encha-Razavi, F., and Chelly, J. (2010). Mutations in the neuronal ss-tubulin subunit TUBB3 result in malformation of cortical development and neuronal migration defects. Hum Mol Genet *19*, 4462-4473.

Poirier, K., Saillour, Y., Fourniol, F., Francis, F., Souville, I., Valence, S., Desguerre, I., Marie Lepage, J., Boddaert, N., Line Jacquemont, M., Beldjord, C., Chelly, J., and Bahi-Buisson, N. (2013). Expanding the spectrum of TUBA1A-related cortical dysgenesis to Polymicrogyria. Eur J Hum Genet *21*, 381-385.

Romaniello, R., Tonelli, A., Arrigoni, F., Baschirotto, C., Triulzi, F., Bresolin, N., Bassi, M.T., and Borgatti, R. (2012). A novel mutation in the beta-tubulin gene TUBB2B associated with complex malformation of cortical development and deficits in axonal guidance. Dev Med Child Neurol *54*, 765-769.

Sohal, A.P., Montgomery, T., Mitra, D., and Ramesh, V. (2012). TUBA1A mutation-associated lissencephaly: case report and review of the literature. Pediatr Neurol *46*, 127-131.

Tischfield, M.A., Baris, H.N., Wu, C., Rudolph, G., Van Maldergem, L., He, W., Chan, W.M., Andrews, C., Demer, J.L., Robertson, R.L., Mackey, D.A., Ruddle, J.B., Bird, T.D., Gottlob, I., Pieh, C., Traboulsi, E.I., Pomeroy, S.L., Hunter, D.G., Soul, J.S., Newlin, A., Sabol, L.J., Doherty, E.J., de Uzcategui, C.E., de Uzcategui, N., Collins, M.L., Sener, E.C., Wabbels, B., Hellebrand, H., Meitinger, T., de Berardinis, T., Magli, A., Schiavi, C., Pastore-Trossello, M., Koc, F., Wong, A.M., Levin, A.V., Geraghty, M.T., Descartes, M., Flaherty, M., Jamieson, R.V., Moller, H.U., Meuthen, I., Callen, D.F., Kerwin, J., Lindsay, S., Meindl, A., Gupta, M.L., Jr., Pellman, D., and Engle, E.C. (2010). Human TUBB3 mutations perturb microtubule dynamics, kinesin interactions, and axon guidance. Cell *140*, 74-87.

Tischfield, M.A., Cederquist, G.Y., Gupta, M.L., Jr., and Engle, E.C. (2011). Phenotypic spectrum of the tubulin-related disorders and functional implications of disease-causing mutations. Curr Opin Genet Dev *21*, 286-294.

Whitman, M.C., Andrews, C., Chan, W.M., Tischfield, M.A., Stasheff, S.F., Brancati, F., Ortiz-Gonzalez, X., Nuovo, S., Garaci, F., MacKinnon, S.E., Hunter, D.G., Grant, P.E., and Engle, E.C. (2016). Two unique TUBB3 mutations cause both CFEOM3 and malformations of cortical development. Am J Med Genet A *170A*, 297-305.

Wu, J., Duggan, A., and Chalfie, M. (2001). Inhibition of touch cell fate by egl-44 and egl-46 in C. elegans. Genes & development *15*, 789-802.

Zanni, G., Colafati, G.S., Barresi, S., Randisi, F., Talamanca, L.F., Genovese, E., Bellacchio, E., Bartuli, A., Bernardi, B., and Bertini, E. (2013). Description of a novel TUBA1A mutation in Arg-390 associated with asymmetrical polymicrogyria and mid-hindbrain dysgenesis. Eur J Paediatr Neurol *17*, 361-365.

Zheng, C., Diaz-Cuadros, M., and Chalfie, M. (2015a). Dishevelled attenuates the repelling activity of Wnt signaling during neurite outgrowth in Caenorhabditis elegans. Proceedings of the National Academy of Sciences of the United States of America *112*, 13243-13248.

Zheng, C., Diaz-Cuadros, M., and Chalfie, M. (2015b). Hox Genes Promote Neuronal Subtype Diversification through Posterior Induction in Caenorhabditis elegans. Neuron *88*, 514-527.

Zheng, C., Diaz-Cuadros, M., and Chalfie, M. (2016). GEFs and Rac GTPases control directional specificity of neurite extension along the anterior-posterior axis. Proceedings of the National Academy of Sciences of the United States of America *113*, 6973-6978.